ELSEVIER

Materials Science and Engineering A361 (2003) 331–337

ENGINEERING A

www.elsevier.com/locate/msea

Lead induced intergranular fracture in aluminum alloy AA6262

O. Wouters, J.Th.M. De Hosson*

Department of Applied Physics, Materials Science Center, The Netherlands Institute for Metals Research, University of Groningen, Nijenborgh 4, 9747 AG Groningen, The Netherlands

Received 18 November 2002; received in revised form 23 June 2003

Abstract

The influence of lead on the fracture behavior of aluminum alloy AA6262 is investigated. Under certain conditions, the mode of fracture changes from transgranular microvoid coalescence to an intergranular mechanism. Three different intergranular fracture mechanisms are observed: liquid metal embrittlement, dynamic embrittlement at temperatures below the melting temperature of lead, and intergranular microvoid coalescence. An attempt is made to examine the dependence of these three mechanisms on temperature, strain rate, and stress state using in situ scanning electron microscopy (SEM). Liquid metal embrittlement occurs when the alloy is fractured at temperatures above the melting temperature of lead and at low strain rates. At lower temperatures, the occurrence of dynamic embrittlement depends largely on strain rate, stress state, and temperature. Intergranular microvoid coalescence is not often observed.

Keywords: Al-alloy AA6262; Fracture; In situ scanning electron microscopy; Dynamic embrittlement; Liquid metal; Pb

1. Introduction

Low concentration heavy metal impurities can cause considerable changes in the mechanical properties of aluminum alloys. These impurities can enter the metal in cost reducing scrap-recycling processes or by diffusional processes, which can be accelerated by elevated temperatures, like liquid metal embrittlement. Sometimes they are also added intentionally. This is the case in the aluminum alloy AA6262. The alloy composition is rather similar to that of the more known AA6061 alloy, i.e. high concentrations of magnesium and silicon that form the strengthening precipitate, Mg_2Si. The main difference is the presence of lead and bismuth, which are added to increase the alloy machinability. The chemical composition of the alloy is: 1.14 at.% Mg, 0.78 at.% Si, 0.30 at.% Fe, 0.13 at.% Cu, 0.06 at.% Mn, 0.06 at.% Cr, 0.08 at.% Pb, 0.07 at.% Bi, and 97.38 at.% Al. Because most of these heavy metal impurities have a very low solubility in aluminum, they have a tendency to segregate towards grain boundaries, free surfaces or heterophase interfaces. There they can cause the fracture resistance of the alloy to change in a number of different ways.

The dominant fracture mechanism in AA6061 is transgranular microvoid coalescence. After extensive deformation, small voids originate near intermetallic particles either due to decohesion at the particle/matrix interface or due to the fracture of the brittle particles themselves. These voids grow as a result of extensive plastic deformation until they coalesce. Due to the presence of lead and bismuth in AA6262 however, other mechanisms may control the fracture process. Bismuth reacts with magnesium to form Bi_2Mg_3, which is stable over a large temperature range. As a result, bismuth is not considered to influence the fracture behavior strongly. The focus of this article therefore will be on the influence of lead, which is present around intermetallic particles and is also found at small grain boundary precipitates.

At temperatures above the melting temperature T_m of lead (327 °C), liquid metal embrittlement can occur. Above this temperature, liquid droplets of lead are present at the grain boundaries. The contact angle θ between the droplets and the aluminum depends on the grain boundary energy σ_{GB}, and the energy of the solid/ liquid interface σ_{SL} according to $\sigma_{GB} = 2\sigma_{SL}\cos\theta$. Because σ_{SL} decreases faster than σ_{GB} with increasing temperature, there is a temperature at which θ becomes zero. This temperature is denoted as T_w, the wetting transition temperature and refers to the temperature at which the boundary is replaced by a layer of the liquid phase, that is complete wetting occurs. The value of T_w

* Corresponding author. Tel.: +31-50-363-4898; fax: +31-50-363-4881.
E-mail address: hossonj@phys.rug.nl (J.Th.M. De Hosson).

0921-5093/$ – see front matter © 2003 Elsevier B.V. All rights reserved.
doi:10.1016/S0921-5093(03)00521-5

depends on the GB energy. Special boundaries have lower energies and are therefore found to have higher values for T_w than random boundaries. For the Al–Pb system, values reported are 560 °C for Σ7 boundaries and 535 °C for a random boundary [1].

Below T_w, the grain boundary is not wetted completely, but the liquid lead is highly mobile and can under the influence of an applied stress assist in the crack forming. Various models have been proposed to explain liquid metal embrittlement. The most commonly accepted is the adsorption-induced reduction in cohesion model [2,3]. When an atom of the liquid metal is adsorbed at the crack tip, electronic rearrangement will cause the strength of the first bond at the crack tip to decrease. After the bond breaks, the embrittling atom is adsorbed at the next bond and the process repeats itself. Since hardly any plasticity is involved in this process, it results in microscopically flat fracture surfaces. Another popular model is the so-called enhanced dislocation emission model [4] in which the effect of the liquid metal atoms is not reducing the tensile cohesive strength, but rather diminishing the shear strength of the bonds. This leads to an enhanced nucleation of dislocations at the crack tip, and failure occurs by localized plasticity, void growth, and coalescence directly in front of the crack tip. Fractography results by Lynch, show intergranular fracture surfaces covered with little dimples [5,6]. The large strains in the precipitate free zones (PFZ) are assumed to promote the occurrence of a microvoid coalescence process over decohesion.

At temperatures below its melting temperature, the lead can still contribute to intergranular brittle fracture. It is well known that high strength alloys can suffer from brittle fracture if they contain a mobile embrittling element on their surface. Under the influence of a high stress and at elevated temperatures, the surface element experiences a driving force for inward diffusion. This is the same force that controls the processes known as Herring-Nabarro and Coble creep [7]. The embrittling element need not be on the surface for this dynamic embrittlement to occur. Upon application of a tensile force, diffusion of the embrittling element from the bulk or from grain boundaries, towards regions of high stress causes a reduction in coherence, which can accelerate failure dramatically [8]. Dynamic embrittlement, being a diffusional process, needs high temperatures and low strain rates. This type of fracture is characterized by a stepwise crack propagation at a very low speed (∼1 μm/s). According to the model proposed by Bika and McMahon [9], this stepwise propagation arises because the small diffusive zone in front of the crack tip only fractures when the impurity concentration in the zone is high enough. After this decohesion, the crack rests until the concentration in the new diffusive zone reaches the critical value for decohesion. Although this mechanism has been demonstrated by microscopic observations of fracture surfaces, which clearly show striations [8,10], other models predict a more continuous form of fracture [11]. Small amounts of lead are shown to cause intergranular fracture in aluminum alloys when tested under very low strain rates ($10^{-6}\,s^{-1}$) or under sustained load conditions at near ambient temperatures [12,13].

During aging of most aluminum alloys, a so-called precipitate free zone originates. Upon deformation, strain will initially be highly localized in these regions and because of strengthening effects, plastic deformation will be enhanced in the interior of the grains. This will result in transgranular fracture. If however the strain in the PFZ is high enough to cause decohesion of the grain boundary precipitates, these voids may coalesce resulting in intergranular microvoid coalescence. It is believed that a high hydrostatic stress promotes the growth of existing voids and thereby increases the changes for intergranular microvoid coalescence to occur [14]. Transmission electron microscopy studies on AA6061 have shown that a heat treatment comparable to the one used in this research results in a large amount of grain boundary precipitation and a PFZ-size of several tenths of nanometers. For elaborate microscopic observations, reference is made to [15].

This paper is aimed at scrutinizing the parameters that govern the occurrence of the above-mentioned fracture mechanisms. To this end, a large number of tensile tests were performed in which the following parameters were varied: temperature, strain rate (crosshead speed), and stress state (sample thickness and notch configuration). The resulting fracture surfaces were studied extensively to make a distinction among the various fracture mechanisms. The objective of the paper is not to produce a full fracture map, but to focus on the various fracture mechanisms by changing the notch configuration also. Indeed, only for unnotched specimens, a strain rate can be derived.

2. Processing route and experimental procedures

The alloys were received in as-extruded condition. To convert the brittle α-intermetallic into the more ductile β-intermetallic and refine its distribution, the following thermomechanical processing route has been followed. First, the samples were homogenized for 6 h at 560 °C, and water quenched. A thickness reduction was achieved by three cold rolling steps alternated with short anneals at 560 °C. The reduction in the last rolling step was 40%. Finally, the alloy was solution heat treated for 15 min at 560 °C and aged for 18 h at 160 °C to achieve a T6 aging condition. Flat tensile specimens were cut from the processed alloy using a high power YAG laser for thin samples (∼1 mm) and spark erosion cutting for thicker sample (2.5 mm). The geometry of the tensile specimens is shown in Fig. 1. This figure shows a specimen with a rounded notch and a specimen with a V-shaped notch. Samples without a notch were also made to vary the stress state.

To deform the specimens, a special tensile stage was used that can be mounted inside a scanning electron microscope (SEM). This offers the possibility to view the surface of

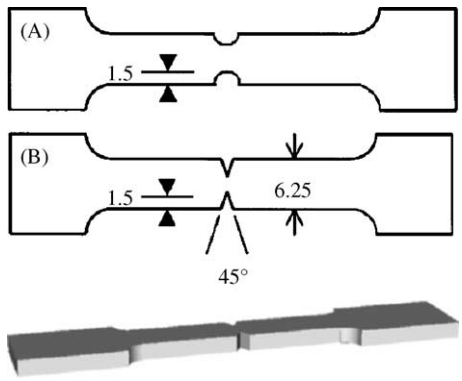

Fig. 1. Geometry of notched tensile specimen. (a) rounded notch; (b) V-shaped notch.

the sample during deformation, and ensures good vacuum conditions, thereby eliminating the occurrence of environment assisted fracture such as stress corrosion cracking. This tensile stage is equipped with a heating element that can heat the sample up to at least 600 °C. The crosshead speed can be varied between 0.2 and 25 μm/s, correspondingly for unnotched specimens with strain rates of 9.5×10^{-6} and $1.2 \times 10^{-3}\,s^{-1}$, respectively. The microscope used for this research is a Philips XL30 FEG environmental SEM. This microscope was also used for the fractography together with a Philips XL30s FEG microscope. The ESEM is equipped with a backscattered electron (BSE) detector, which is very useful for imaging small amounts of lead, because of its much higher atomic weight. The XL30s FEG is equipped with a special electromagnetic lens, which gives the possibility of ultra high-resolution imaging.

3. Results

First, we concentrate on the effect of the temperature during deformation. Fig. 2 shows the stress–strain characteristics of a series of tensile tests performed at different temperatures. These samples all had a thickness of 1.2 mm and a V-shaped notch. The crosshead speed was set to the lowest possible value (0.2 μm/s) to allow diffusion controlled fracture mechanisms to occur. At room temperature, the tensile strength is 520 MPa. When the temperature is raised to 100 or 300 °C, a small drop in tensile strength is observed. If the temperature is raised further to 400 °C or higher, the curves collapse totally. An additional test performed at 600 °C, showed fracture immediately at the onset of straining.

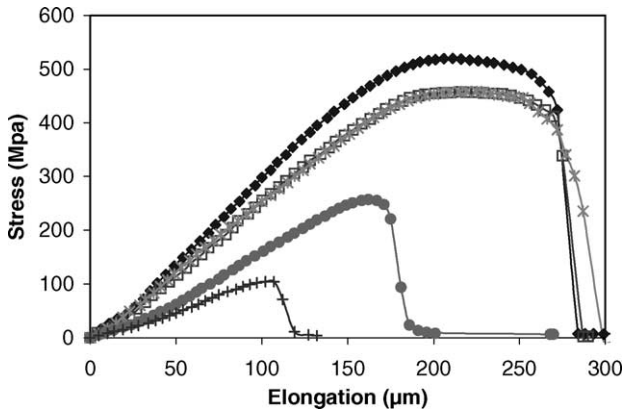

Fig. 2. Stress–strain curves of thin V-notched specimen fractured at different temperatures. (◆) 25 °C; (□) 100 °C; (✱) 300 °C; (●) 400 °C; (+) 550 °C.

SEM images of the fracture surfaces resulting from the above-mentioned tests are shown in Fig. 3. As observed in the graphs of Fig. 2, the fractography results also show a clear distinction between the samples fractured above 400 °C and those fractured below. In the latter samples, the fracture surfaces are covered with large dimples indicating a ductile transgranular mode of fracture (Fig. 3(a)). The samples fractured at 400 °C or above show an intergranular fracture surface with smooth grain facets indicating little or no plasticity (Fig. 3(b)).

When the samples are subjected to a closer examination, more differences can be distinguished. All the samples that fracture predominantly in a transgranular way show also some regions of intergranular fracture, which are always located close to the notch. In the room temperature samples, these regions are very rarely seen, but with increasing temperature, they are observed more frequently. Especially on the fracture surfaces of the samples fractured at 300 °C, large intergranular parts are present close to the notches. The surface of these intergranular regions has roughness more than the samples fractured at higher temperatures, and it is covered with little particles, which are brighter in the BSE image, indicating that these are lead particles (Fig. 3(c) and (d)). In Fig. 4, a comparison is made between the surfaces of grains that have fractured intergranularly at temperatures 300, 400, and 600 °C, respectively. At a fracture temperature of 600 °C, most grain facets are flat like the ones in Fig. 4(c). The small deformation shown in Fig. 4(b) is also found in this sample, but is more abundant in the samples fractured at 400 °C. The samples fractured at 300 °C show a much rough fracture surface. Incidentally, clear striations show up as shown in Fig. 4(a), but also at the top grain in Fig. 3(c).

Finally, in the low temperature samples, a few regions of ductile intergranular fracture could be found. These localized regions are found not only close to the notch, but only a few grains show the dimpled intergranular surface shown in Fig. 3(e).

To examine the influence of the stress state, the thickness of the samples was changed. The thinner samples (1.2 mm) break in a slanting way indicating plane stress conditions. The thicker samples (2.5 mm) break in a flat way, indicating plane strain conditions. The general fracture characteristics of both the types of samples are similar. In the thinner samples however, slightly more brittle intergranular fracture was found at temperatures below 400 °C. The second

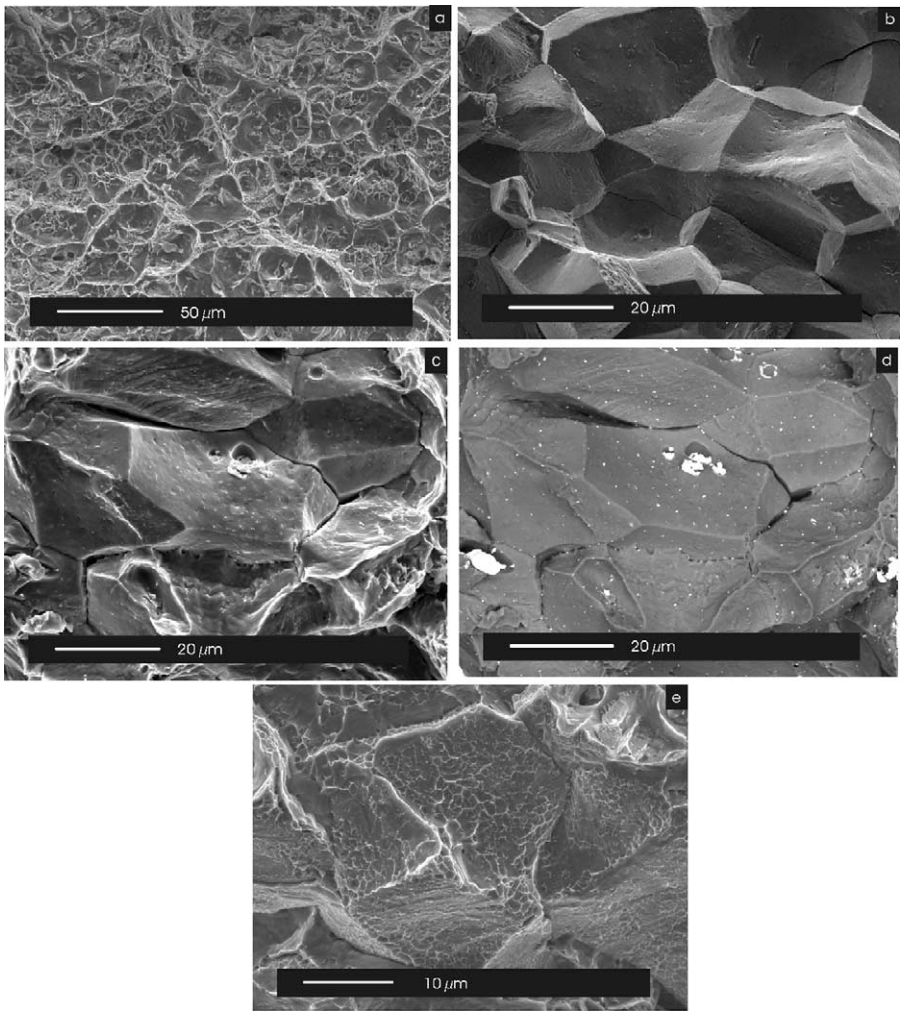

Fig. 3. Typical fracture surfaces. (a) Transgranular microvoid coalescence; (b) brittle intergranular fracture at high temperatures; (c) intergranular fracture at $T < T_m$; (d) as (c), but using BSE detector showing lead particles; (e) intergranular fracture showing ductility in the form of dimpled facets.

method to vary the stress state is to apply different notch geometries. Three different geometries are compared: samples without a notch, samples with a V-notch, and samples with rounded notches. Samples of these types were fractured at room temperature, 300, and 550 °C. Differences were only observed in the sample fractured at 300 °C. Specimens without a notch, fracture transgranularly, whereas samples with a V-notch show incidental intergranular parts. The specimens with rounded notches however, fracture in the region of the notch almost completely intergranularly (see Fig. 5(a)). Only one configuration resulted in a complete intergranular fracture at 300 °C. This was a thin sample (1.2 mm) with a rounded notch, which was fractured at the lowest possible strain rate.

The strain rate was altered by varying the crosshead speed of the tensile stage. The two extreme values of the stage were used, i.e. 0.2 and 25 μm/s. Because the samples with rounded notches which fractured at 300 °C showed a large amount of intergranular fracture, this configuration was used to test the influence of the higher crosshead speed. The low and high strain rate results are compared in Fig. 5. Fig. 5(a) shows predominantly intergranular failure in the notch region after slow fracturing. In Fig. 5(b), showing the result of fast fracture, only ductile transgranular failure is present. At higher temperatures, the effect of strain rate is even more pronounced. In Fig. 6, the fracture surfaces of two thick V-notched samples fractured at 450 °C are compared. Fig. 6(a) corresponds to a crosshead speed of 0.2 μm/s and Fig. 6(b) to a crosshead speed of 25 μm/s. The first sample breaks completely intergranularly and the second completely transgranularly. At a temperature of 550 °C, the strain rate has no effect anymore. All the specimens at this temperature break intergranularly.

4. Discussion

As expected, a large number of different fracture surfaces were observed, when the parameters governing the deformation were altered. It is believed that the three

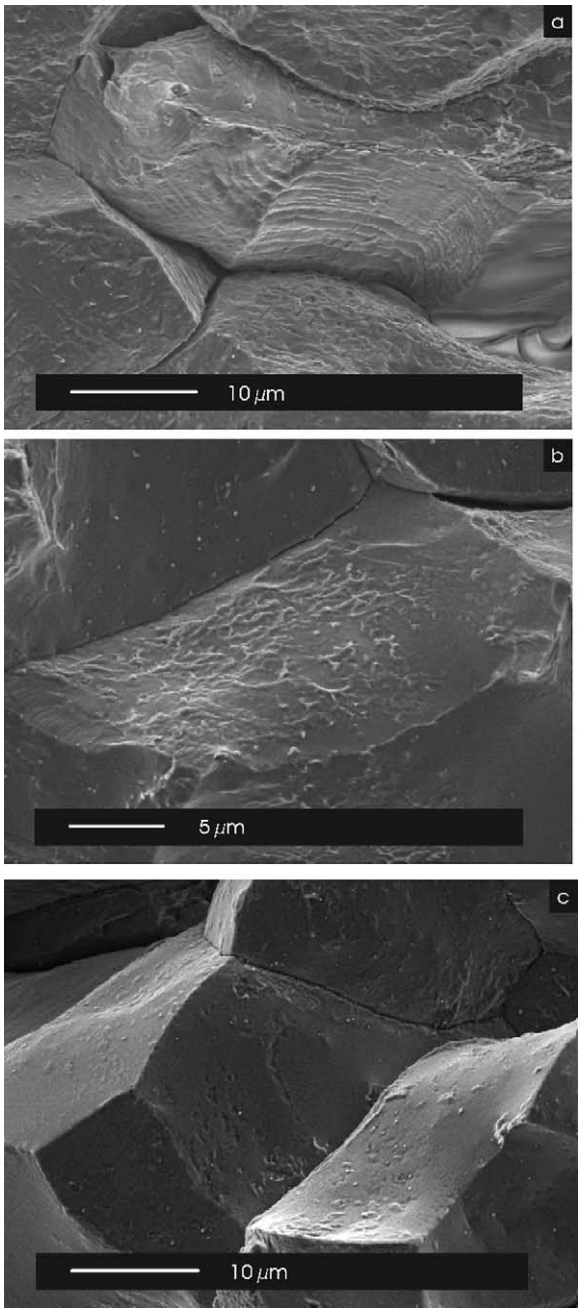

Fig. 4. Fracture surfaces of lead-induced intergranular fracture produced at (a) 300 °C; (b) 400 °C; (c) 600 °C showing clear differences in roughness.

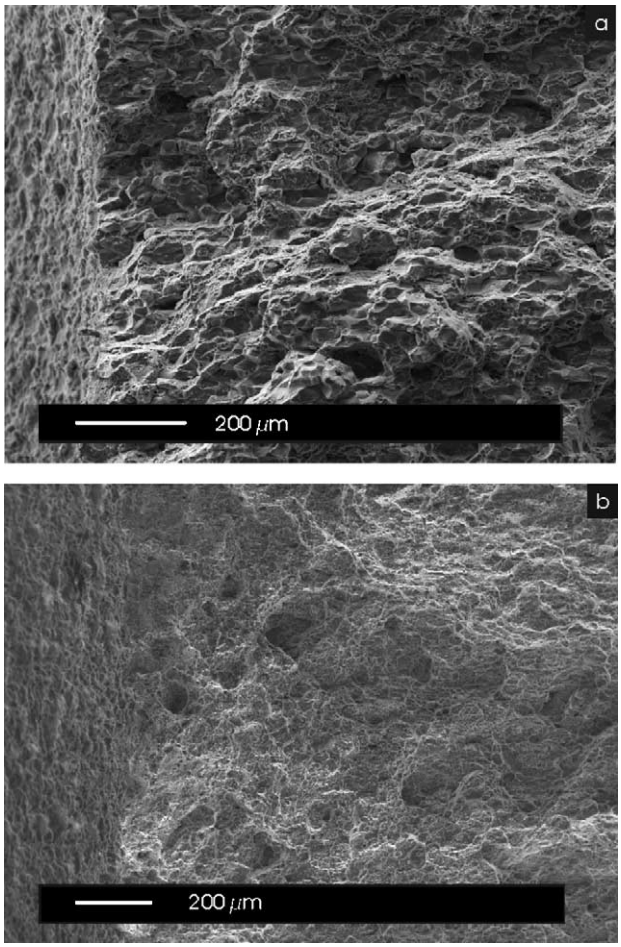

Fig. 5. Fracture surfaces showing the effect of strain rate on dynamical embrittlement at $T < T_m$. (a) A crosshead speed of 0.2 μm/s leads to large regions of intergranular fracture and (b) a crosshead speed of 25 μm/s results in transgranular fracture.

intergranular fracture mechanisms described at the beginning of this paper all take place at some point during our experiments.

At temperatures above the melting temperature of lead, the tensile tests performed at the lowest possible strain rate result in complete intergranular failure. At higher strain rate, only the specimens fractured at much higher temperatures break intergranularly. This supports the theory that only at temperatures far above T_m, complete wetting occurs. Our set-up is not suitable for a precise determination of this wetting transition temperature, but it is clear that only the specimens fractured at 550 and 600 °C, were wetted completely. All other specimens needed a certain amount of straining before the grains started to decohere. At temperatures between T_m and T_w, the lead is a liquid, but does not wet the boundary. Still stress-assisted diffusion and therefore time is needed to cause failure. Even at 450 °C, the propagation of the crack, when strained at 25 μm/s, occurs at such a high velocity that there is no time for the liquid metal to diffuse towards the crack tip and assist in the crack growth.

The differences between the fracture surfaces shown in Fig. 4(b) and (c), is another indication that at 400 °C, the lead is not wetting the boundary. The roughness shown in Fig. 4(b) proves that some plastic deformation has taken place. Because this plasticity is very shallow, it is likely to be confined to the PFZ.

At temperatures below T_m, under certain conditions, a similar kind of brittle fracture takes place. Because the lead is no longer a liquid, this process can be described as solid metal embrittlement. Following the aforementioned

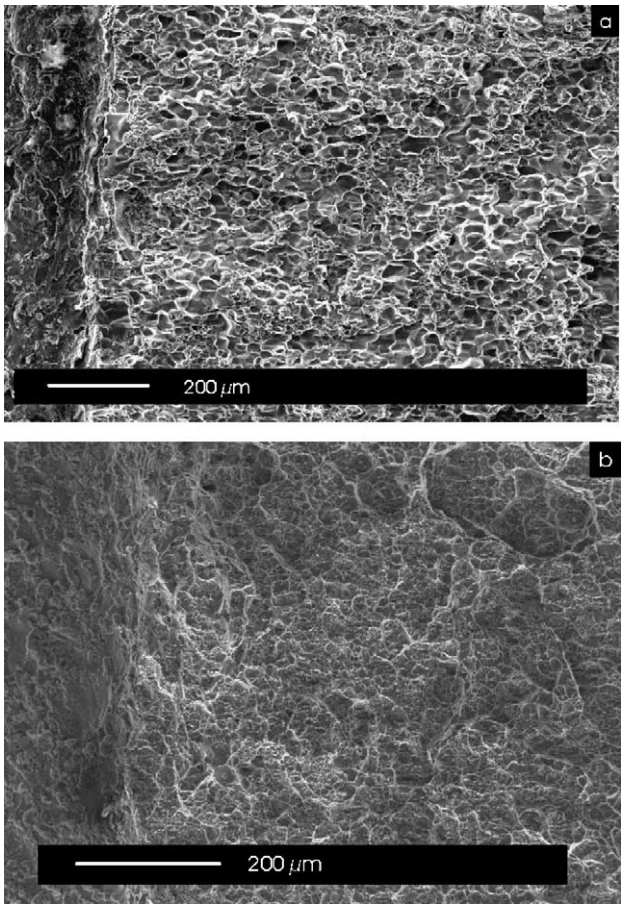

Fig. 6. Fracture surfaces showing the effect of strain rate on liquid metal embrittlement. (a) A crosshead speed of 0.2 μm/s leads to large regions of intergranular fracture and (b) a crosshead speed of 25 μm/s results in transgranular fracture.

argument, dynamic embrittlement can only occur at low strain rates and elevated temperatures. When the crosshead speed in our experiments was raised to 25 μm/s, no dynamic embrittlement was observed. At the lowest strain rate, traces of dynamic embrittlement were mostly observed in the notch region of the fracture surface. In the specimens without a notch, no dynamic embrittlement was observed at all. This is in accordance with the idea that a high stress for a prolonged time is a prerequisite for dynamic embrittlement to occur. Although a rounded notch possesses a lower stress intensity factor than a V-shaped notch, it produces the largest amount of dynamic embrittlement observed in our experiments. With this configuration, the hydrostatic pressure is the highest in the center of the tensile specimen and not near the notches in the V-shaped notch. A high hydrostatic pressure, promotes the nucleation and growth of voids, and therefore the occurrence of transgranular fracture by microvoid coalescence. Because hydrostatic stresses are much higher in the thicker samples (i.e. under plane strain conditions), dynamic embrittlement is observed to a lesser extent. These results need not be inconsistent with the view that a high triaxility is a prerequisite for dynamic embrittlement, but they strongly suggest that transgranular microvoid coalescence is the more dominant failure mechanism.

Locally, some parts showing pronounced striations are found (Fig. 4(a)). Although literature links dynamic embrittlement with the occurrence of striations, in our case they are observed only rarely. Possibly, the dimensions of the striations are such that they are not easily resolved with the SEM. Another explanation might be that plasticity in the soft PFZ is interfering with the lead-induced fracture, causing the fracture surface to appear somewhat smoothened. It is anticipated that other lead containing alloys, whether the lead is added intentionally or is just present as unwanted impurity, experience failure by dynamic embrittlement after prolonged loading at elevated temperatures, i.e. under creep circumstances.

Although sporadically arising, intergranular microvoid coalescence does not seem to be of great influence on the macroscopic fracture behavior of the alloy, traces of intergranular microvoid coalescence is found in most of the fractured samples, except in those samples that fracture in a completely brittle manner (high temperatures). Because only a few grains show the dimpled facets, we suggest that only under specific conditions, intergranular microvoid coalescence is the preferred fracture mechanism.

5. Conclusions

Although lead is added to the AA6262 alloy to enhance its performance at high strain rate operations (i.e. to increase its machinability), it can have a detrimental effect on the low strain rate fracture characteristics. At temperatures above the melting temperature of lead, the alloy is susceptible to liquid metal embrittlement. At temperatures below the wetting transition temperature, intergranular decohesion is a stress-assisted process, requiring low strain rates. This results in a small increase in roughness of the grain facets, when compared with the smooth fracture surfaces produced above T_w. At these temperatures, fracture is almost imminent at the onset of a tensile stress and independent of strain rate.

Below the melting temperature, the lead atoms are under certain circumstances mobile enough to cause stress-induced intergranular decohesion. This dynamic embrittlement occurs only when some initial stress localizers (notches) are present. The amount of dynamic embrittlement depends strongly on both temperature and strain rate. Thinner samples and rounded notches produce more dynamic embrittlement than thicker samples and V-shaped notches, because under the latter circumstances the hydrostatic pressure is high, which promotes the occurrence of a void growth and coalescence fracture mechanism.

Intergranular void growth and coalescence does not occur frequently, and its presence does not appear to be highly dependent on one of the experimental parameters investigated.

Acknowledgements

The Foundation for Fundamental Research on Matter (FOM-Utrecht) and the Netherlands Institute for Metals Research are acknowledged for their financial support.

References

[1] D.A. Molodov, G. Gottstein, U. Czubayko, L. Shvindlerman, Phys. Met. Metall. 83 (1997) 408–416.
[2] A.R.C. Westwood, M.H. Kamdar, Philos. Mag. 8 (1963) 787–804.
[3] N.S. Stoloff, T.L. Johnston, Acta Metall. 11 (1963) 251–256.
[4] S.P. Lynch, Mater. Forum 11 (1988) 268–283.
[5] S.P. Lynch, Acta Metall. 29 (1981) 325–340.
[6] S.P. Lynch, J. Mater. Sci. 20 (1985) 3329–3338.
[7] C.J. McMahon Jr., J.A. Pfaendtner, R.C. Muthiah, Czechoslovak J. Phys. 45 (1995) 230.
[8] D. Bika, J.A. Phaendtner, M. Menyhard, C.J. McMahon Jr., Acta Metall. Mater. 43 (1995) 1895–1908.
[9] D. Bika, C.J. McMahon, Acta Metall. Mater. 43 (1995) 1909–1916.
[10] R.D.K. Misra, Scripta Mater. 35 (1996) 1347–1352.
[11] Y. Xu, J.L. Bassani, Mater. Sci. Eng. A 260 (1999) 48–54.
[12] J.J. Lewandowski, V. Kohler, N.J.H. Holroyd, Mater. Sci. Eng. 96 (1987) 185–195.
[13] J.J. Lewandowski, Y.S. Kim, N.J.H. Holroyd, Metall. Trans. A 23 (1992) 1679–1689.
[14] T. Pardoen, D. Dumont, A. Deschamps, Y. Brechet, J. Mech. Phys. Sol., submitted for publication.
[15] M. De Haas, J.Th.M. De Hosson, J. Mater. Sci. 37 (2002) 5065–5073.